Sky Exposure Mapping with Preconditioned Spherical Generalized Additive Model

Zsolt Bagoly[1]

[1] Ludovika University of Public Service, Budapest

Collaborators: L.G. Balazs, I. Horvath, A. Joo, S. Pinter, I. Racz, L.V. Toth

A matematika és a fizika időszerű kérdései 2026 - Nemzetközi tudományos konferencia

Universe 2024,10(4),185; *Universe* 2026,12,31B. ++

Outline

Gamma-Ray Bursts as Cosmological Tracers

Key Properties

- GRBs are the most luminous electromagnetic events in the Universe.
- They trace the star formation rate (SFR) up to very high redshifts ($z \approx 9$).
- Unlike galaxy surveys (e.g. SDSS, LSST), GRBs are not limited by local extinction except in the optical channel.

High-Redshift Advantages

- GRBs provide a probe of the ”Dark Ages” and the Epoch of Reionization.
- Their detection is nearly independent of the foreground interstellar medium (ISM) in the gamma-ray band.

The Cosmological Principle and Structures observed by GRBs

Theoretical Basis

- The Universe is assumed to be homogeneous and isotropic on large scales.
- Transition to homogeneity scale: $R_{hom} \approx 260h^{-1}$ Mpc.

The Observational Conflict

- Detection of structures exceeding 1 Gpc in size.
  - **The Hercules-Corona Borealis Great Wall:** A massive cluster spanning ≈ 3 Gpc.
  - **The Giant GRB Ring:** A circular structure with diameter ≈ 1.7 Gpc.
  - **The Large Quasar Groups:** Giant Quasar Arc has a size of ≈ 1.2 Gpc.
- These structures question the fundamental assumptions of FLRW cosmology.

Problem of Observational Bias

The density of tracers (GRBs) is modulated by the uneven sky exposure of satellites and ground-based telescopes.

The Cosmological Principle and Structures observed

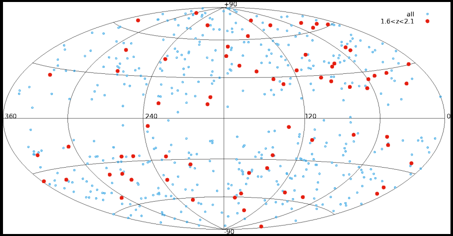

HER-CB Great Wall MNRAS.452.3.2236

edi

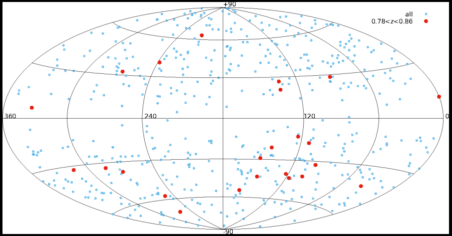

Giant GRB Ring MNRAS.452.3.2236

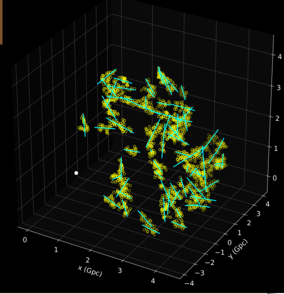

LQG MNRAS.511.3.4159

- **The Hercules-Corona Borealis Great Wall:** A massive cluster spanning ≈ 3 Gpc.
- **The Giant GRB Ring:** A circular structure with diameter ≈ 1.7 Gpc.
- **The Large Quasar Groups:** Giant Quasar Arc has a size of ≈ 1.2 Gpc.

- These structures question the fundamental assumptions of FLRW cosmology.

Problem of Observational Bias

The density of tracers (GRBs) is modulated by the uneven sky exposure of satellites and ground-based telescopes.

Selection Function Reconstruction

The observed GRB distribution in the redshift sample is a combination of:

- **Physical Clustering:** Any actual cosmic structure.
- **Satellite Dynamics:** The Sky Exposure Function (e.g., Swift BAT pointing).
- **Ground Constraints:** Optical follow-up efficiency (weather, telescope time).

Goal: determine a mathematically solid and physically consistent map of the $\lambda_z(\mathbf{x})$ Sky Exposure Function

- Distinguish between physical clustering and instrumental artifacts.
- Can provide weights for luminosity function and rate density calculations.
- Check for any correlation between the exposure factor and a measured physical parameter (flux, fluence, T_{90}, etc.).

The Swift BAT Catalog

Neil Gehrels *Swift* Observatory

- **Energy Range:** $15 - 150$ keV (BAT).
- **Total Sample (*N_{total}*):** 1665 GRBs (2004–2022), 427 GRBs with *spectroscopic* redshifts (up to Aug 2022).
- Coordinates: UKSSDC provides refined coordinates using the XRT detector. Typical error: $\approx 1 - 2$ arcseconds.
- Enhanced XRT positions where they exist, otherwise BAT.
- Different operational time-scales and sensitivities.
- Sky distribution is affected by Galactic extinction and satellite pointing.

The Swift BAT GRB Redshift Sample

Category	**Count**
Total Triggers (N_{total})	1665
Redshift Sample (N_z)	427
- Rapid Afterglow	300
- Host Galaxy	127

- Photometric redshifts and limits were excluded to ensure precision (forthcoming radial/3D analysis).
- Redshift range: $0.003 < z < 8.2$, Median redshift: $\langle z \rangle \approx 2.1$.
- Afterglow: High-speed response, limited by weather.
- Host Galaxy: High-exposure, limited by telescope magnitude limits.
- The sample could be used for large-scale structure mapping if the selection function is known.

The Spectroscopic Bottleneck

The Redshift Problem

- Detecting a GRB is easy (gamma-rays); measuring its distance is hard (spectroscopy).
- Only $\approx 25\%$ of Swift GRBs have a measured redshift.

This ”thinning” of the sample is not uniform on the sky!

Selection Effects: A Multidimensional Problem

- **Trigger Efficiency:** Energy dependence of the detector.
- **Localization Efficiency:** Accuracy of X-ray afterglow detection, sky coverage, and observational constraints.
- **Spectroscopic Efficiency:** Visibility of emission/absorption lines.
- **Observational Efficiency:** Access to the telescopes/equipment, determined observers.

The Spectroscopic Bottle

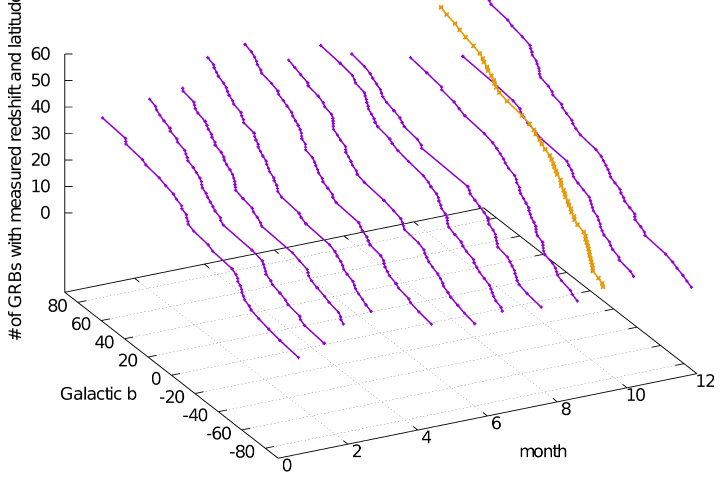

The Redshift Problem

- Detecting a GRB is easy (gar (spectroscopy).
- Only $\approx 25\%$ of Swift GRBs ha

This "thinning" of the sample is r

Selection Effects: A Multidimens

- **Trigger Efficiency:** Energy d
- **Localization Efficiency:** Acc observational constraints.
- **Spectroscopic Efficiency:** Visibility of emission/absorption lines.
- **Observational Efficiency:** Access to the telescopes/equipment, determined observers.

Dedicated optical campaigns around October!

Kernel Density Estimation (KDE) Principles

General KDE Formula:

$$\hat{f}_h(x) = \frac{1}{nh} \sum_{i=1}^{n} K\left(\frac{x - X_i}{h}\right)$$

- n: number of data points
- h: bandwidth (smoothing parameter)
- $K(\cdot)$: kernel function

- Non-parametric method to estimate the Probability Density Function (PDF) of a random variable from a finite data sample.
- Places a kernel function (a smooth, symmetric function) at each data point and sums them to form the density estimate.

Kernel Density Estimation (KDE) Principles

General KDE Formula:

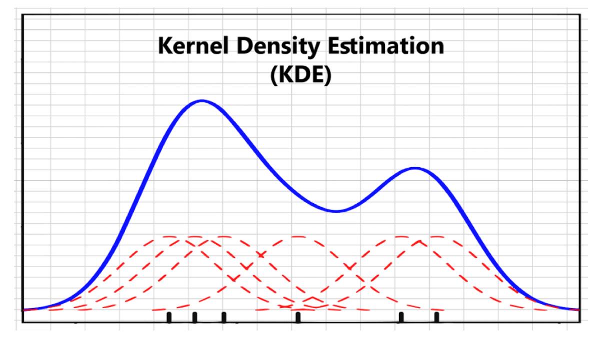

- n: number of data points
- h: bandwidth (smoothing p
- $K(\cdot)$: kernel function

>>

- Non-parametric method to estimate the Probability Density Function (PDF) of a random variable from a finite data sample.
- Places a kernel function (a smooth, symmetric function) at each data point and sums them to form the density estimate.

The Bandwidth Dilemma

Bias-Variance Tradeoff:

The choice of bandwidth h is central in KDE.

- Small h: undersmoothed, wiggly estimate (high variance, low bias).
- Large h: oversmoothed, featureless estimate (low variance, high bias).

It is important to find an optimal h that balances bias and variance. h is more important than the exact shape of the kernel!

Adaptive KDE (AKDE)

- Uses variable bandwidth based on pilot density $\tilde{f}(\mathbf{x})$
- Even with adaptation, the minimum bandwidth is limited by sample size: $h \propto n^{-1/6}$.
- Sparse samples ($N_z = 427$) impose a "soft ceiling" on resolution, acting as a low-pass filter.

Observed Sky Distribution

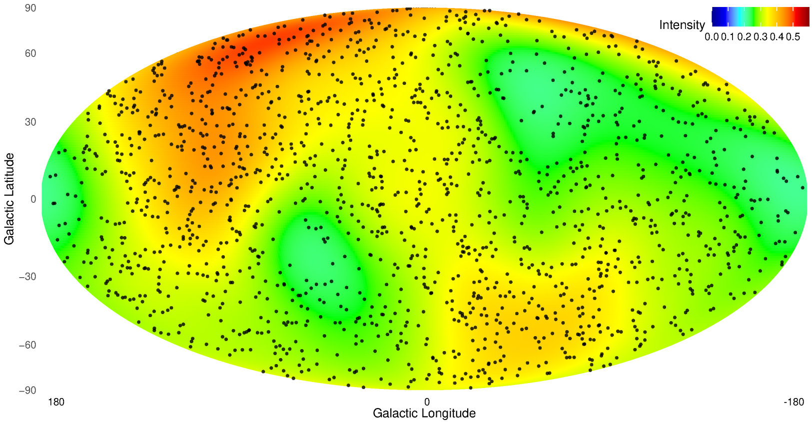

Adaptive KDE estimation of $\hat{\lambda}_{total}(\mathbf{x})$ events' density for the entire Swift BAT population ($N = 1665$). Black points indicate individual GRB positions. The density follows the Swift pointing strategy (equatorial avoidance and orbital geometry).

Bayesian Preconditioning (The Factorized Model)

Factorized Density Estimation

Formulate the problem as estimating a **conditional probability** within a Bayesian framework.

$$\lambda_z(\mathbf{x}) = \lambda_{total}(\mathbf{x}) \times P(z|\mathbf{x})$$

- $\lambda_{total}(\mathbf{x})$: Estimated from a high-statistics sample ($N = 1665$) of all BAT bursts.
- $P(z|\mathbf{x})$: The completeness probability, modeled via Logistic Regression.

Advantages:

- The probability is strictly bounded $P \in [0, 1]$.
- Uses the full catalog as a sky exposure prior (Preconditioning).
- Prevents "leakage" into unobserved regions (e.g., Galactic plane).

Generalized Additive Models (GAM)

We treat redshift measurement as a binary classification problem:

$$y_i \in \{0, 1\} \quad \text{(No Redshift / Redshift)}$$

Logistic Regression on the Sphere

We use a GAM with a Logit Link function to map the linear predictor $\eta(\mathbf{x})$ to probability $p(\mathbf{x})$:

$$\eta(\mathbf{x}) = \ln\left(\frac{p(\mathbf{x})}{1 - p(\mathbf{x})}\right)$$

- $\eta(\mathbf{x})$ is a smooth function on the sphere.
- The logit link ensures $p(\mathbf{x})$ remains physically valid.
- Consistent with Maximum Entropy principles.

Splines on the Sphere (SOS)

Avoiding Grid Artifacts

Pixel-based methods (HEALPix) or planar projections suffer from pole singularities or discretization noise.

Splines on the Sphere

Basis Functions: Wahba's spherical spline basis. The basis is derived from the Green's function of the spherical Laplacian operator, (r is the geodesic distance on $\mathbb{S}^2$):

$$\psi(r) = \frac{1}{4\pi}\left[\ln\left(\sin\frac{r}{2}\right) + \frac{1}{2} - \frac{1}{2}\ln 2\right]$$

- **Isotropic:** Depends only on geodesic distance r, invariant to rotation (k spline support points from k-means clustering).
- **Continuous:** Allows sub-pixel resolution and avoids pole artifacts.
- **Pole Independence:** No singularities at the North or South poles.
- **Efficiency:** Allows analytical calculation of the penalty matrix.

Regularization: Restricted Maximum Likelihood

How to determine the optimal smoothness?

Penalized Likelihood

$$\mathcal{L}_p(\boldsymbol{\beta}) = \mathcal{L}(\boldsymbol{\beta}) - \frac{1}{2}\lambda\boldsymbol{\beta}^T\mathbf{S}\boldsymbol{\beta}$$

- **S**: Penalty matrix determined by surface curvature bending energy, $\int_{\mathbb{S}^2}(\Delta_{\mathbb{S}^2}f)^2 d\Omega$.
- λ: Smoothing parameter, high curvature surfaces are penalized.

REML (Restricted Maximum Likelihood):

- Objectively estimates λ by maximizing the marginal likelihood (integrating out β).
- Robust against overfitting and autocorrelation.
- Equivalent to integrating out the coefficients $\boldsymbol{\beta}$ in a Bayesian framework, maximizing Bayesian Evidence with Gaussian priors.

Akaike Information Criterion (AIC): Information Theoretic Rationale

The k complexity (the basis dimension of the spline) is selected via the AIC.

- AIC measures the Kullback-Leibler distance to the ”true” distribution.
- $AIC = -2\mathcal{L} + 2 \cdot EDF$

  EDF is the Effective Degrees of Freedom defined by the trace of the penalty matrix; it measures how much each data point contributes to its own prediction.

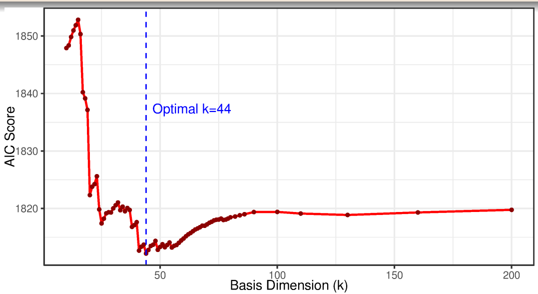

AIC vs. basis dimension k. The global minimum defines the optimal balance.

Reconstructed Completeness Map $P(z|\mathbf{x})$

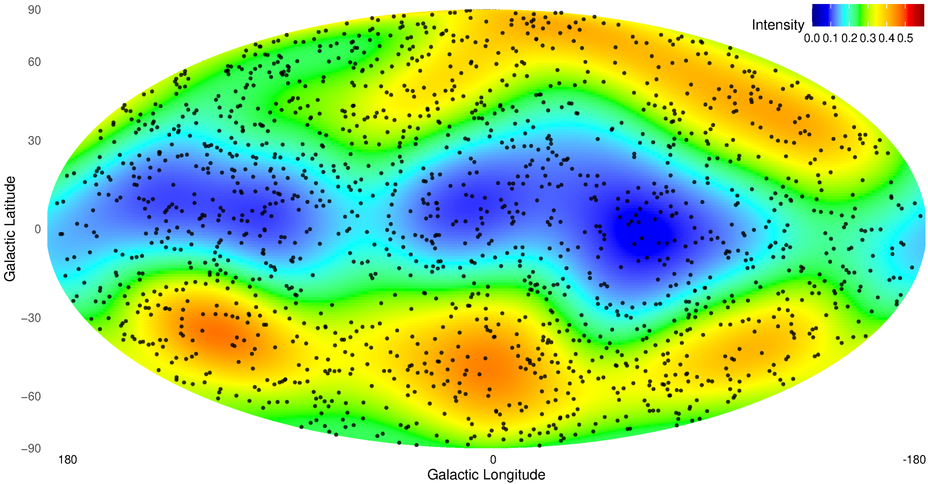

The Bayesian relative probability map $P(\text{Redshift}|\mathbf{x})$. Note the deep suppression around the Galactic plane ($b \approx 0$).

The Precon Probability Map

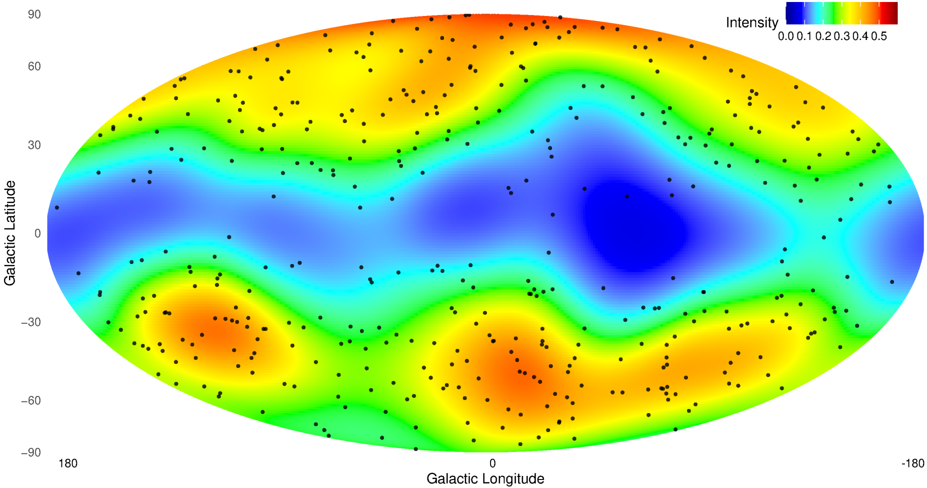

Preconditioned density estimate $\lambda_z(\mathbf{x}) = \lambda_{total}(\mathbf{x}) \times P(z|\mathbf{x})$. Note the sharp definition of the Galactic Plane, recovered despite the sparse redshift sample (very few GRBs with redshift there).

Theoretical Framework: Bandwidth Extension via Preconditioning

The Bandwidth Limit

Standard AKDE bandwidth scales as: $h_{opt} \propto n^{-1/6}$
For small N_z, h is large, acts as a **Low-Pass Filter**, erasing high-frequency features.

Factorized Estimator as Bandwidth Extender

$$\lambda_z^{(Precon)}(\mathbf{x}) = \lambda_{total}(\mathbf{x}) \times P(z|\mathbf{x})$$

- $\lambda_{total}(\mathbf{x})$: Derived from $N_{total} = 1665$ with AKDE (High Bandwidth).
- $P(z|\mathbf{x})$: Derived from sparse binary set N_{total} with redshift selection (Low Bandwidth).
- Recovers finer ('wideband') sky exposure features in $\lambda_z^{(Precon)}(\mathbf{x})$ better than AKDE alone.
- It uses the high-resolution exposure prior to resolve features theoretically invisible in the sparse sample.
- Multiplying two low frequency signals can produce a higher frequency, e.g.: $2 \sin \omega t \cos \omega t \rightarrow \sin 2\omega t$

Theoretical Framework: Information Theoretic Perspective

Minimizing Kullback-Leibler (KL) divergence

$$D_{KL}(\lambda||\hat{\lambda}) = \int_{\mathcal{S}} \left(\lambda(\mathbf{x}) \ln \frac{\lambda(\mathbf{x})}{\hat{\lambda}(\mathbf{x})} - \lambda(\mathbf{x}) + \hat{\lambda}(\mathbf{x}) \right) d\mathbf{x}$$

Minimizing the KL divergence is asymptotically equivalent to maximizing the likelihood of the observed data.

The error decomposes additively:

$$D_{KL}(\lambda_z||\hat{\lambda}_z^{(Precon)}) \approx \underbrace{D_{KL}(P(z|\mathbf{x})||\hat{P}(z|\mathbf{x}))}_{\text{Redshift Effect Estimation Error}} + \underbrace{\int_{\mathcal{S}} P(z|\mathbf{x}) D_{KL}(\lambda_{BAT}(\mathbf{x})||\hat{\lambda}_{BAT}(\mathbf{x})) d\mathbf{x}}_{\text{BAT Exposure Map Reconstruction Error}}$$

- Minimizes the error for Efficiency ($P(z|\mathbf{x})$) using the sparse binary dataset.
- Minimizes the error for the Exposure Map (λ_{total}) using the full large dataset.
- Lower total information loss compared to direct estimation on the sparse subset.

Precon-AKDE Tests: Likelihood Results

Compare the log-likelihood of the observed GRB events for both density maps. Higher values indicate that Precon correctly concentrated a significant portion of the probability mass on the areas where the events actually occur.

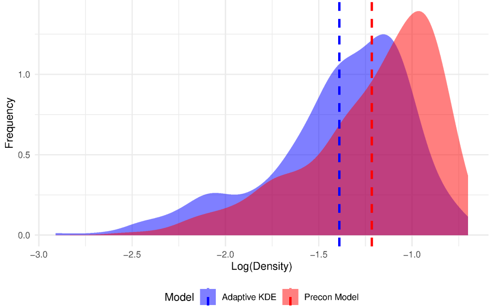

$$\Delta\mathcal{L} = 2(\mathcal{L}_{Precon} - \mathcal{L}_{KDE}) \approx 148.6 \rightarrow \text{Bayes Factor } > 10^{30}$$

Precon better describes the physical event generation process!

Area Under the Receiver Operating Characteristic Curve (AUC/ROC)

Compare the Precon Model vs. Standard Adaptive KDE for the redshift selected GRBs.

AUC is equivalent to the normalized Wilcoxon-Mann-Whitney rank-sum test statistic.

- Invariant to absolute probability calibration.
- Evaluates the sorting of the sky exposure da
- Likelihood that a random event is assigned a higher predicted density than a random background coordinate.
- Continuously scans a threshold for True/False Positive Rate (% of actual Signal/Simulated Background points above the threshold)

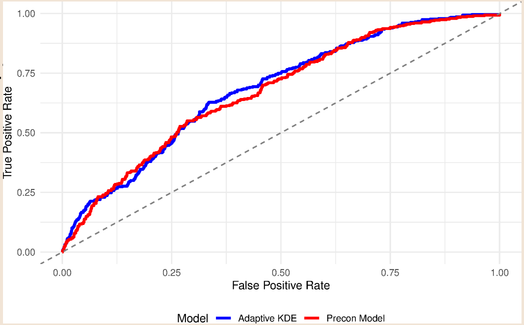

ROC curves are nearly identical (AUC ≈ 0.74).

- AKDE overfits noise, creating ”spikes” exactly at data points.

  This fits noise points/boosts rank (good AUC) but fails in empty regions (bad Likelihood). A map of Dirac deltas on events has AUC=1.0 but is useless.

Artifact Identification: AKDE-Precon Difference Map

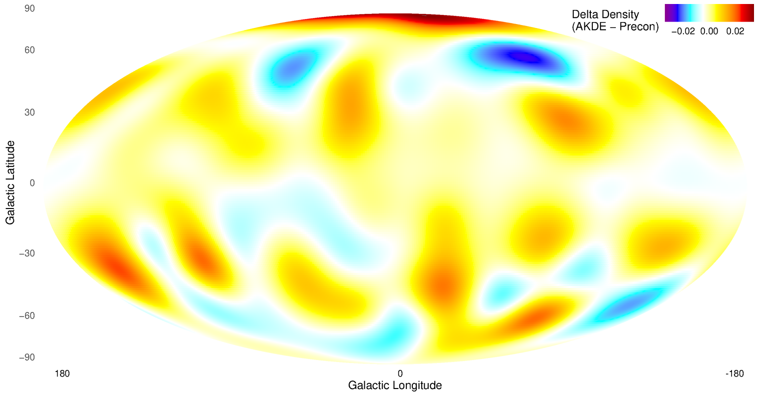

- Identifies ”spurious hot spots” in AKDE that are not supported by the exposure prior.
- AKDE ”leaks” density into the unobserved Galactic Plane.
- Precon uses the prior to ”clamp” the density to zero in known absorption zones.
- This results in a physically correct reconstruction.

Are the Subpopulation Probability Maps Compatible?

Different Observational Biases in Subgroups

- **Afterglow:** Rapid response, sensitive to atmospheric conditions and daytime triggers. Prompt access of the telescopes/observers/equipment/TOO is important!
- **Host Galaxy:** Delayed observation, sensitive to galaxy brightness and stellar crowding in the Galactic Plane. High-exposure, limited by telescope magnitude limits. Sometimes years/decades later than the gamma detection, observational campaigns are common!

The observational timeline is totally different!

Afterglow: $N = 300$, Host Galaxy: $N = 127$.

If Afterglow and Host Galaxy redshift samples have different sky distributions, a unified map is systematically biased.

Are the Subpopulation Pr

Different Observational Biases in

- **Afterglow:** Rapid response, triggers. Prompt access of th !
- **Host Galaxy:** Delayed obser crowding in the Galactic Plan limits. Sometimes years/dec campaigns are common!

The observational timeline is tota

Afterglow: $N = 300$, Host Ga

If Afterglow and Host Galaxy red map is systematically biased.

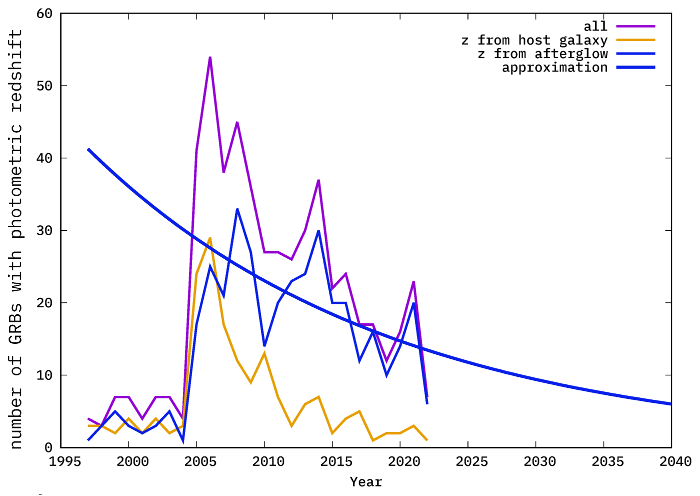

Observation timeline is *different* for Host Galaxy/Afterglow groups!

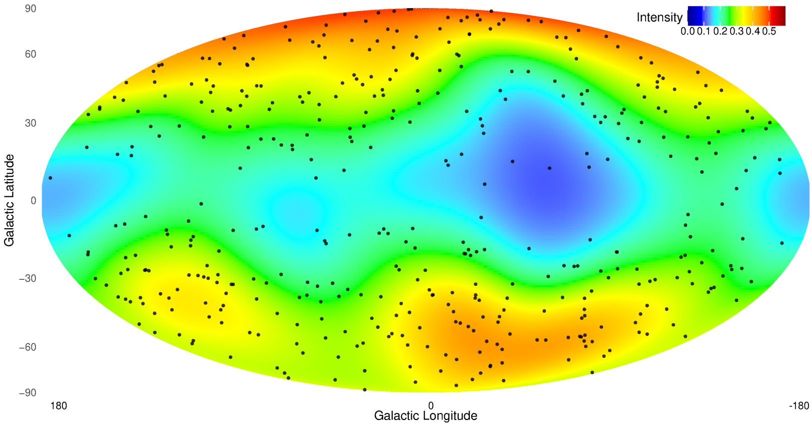

Superposition of the two independent sub-models.
$\Delta\mathcal{L} \approx -16.1$
Lumped model is better; the Split model is statistically inferior because of overfitting.

The Lumped Probability Map (compare!)

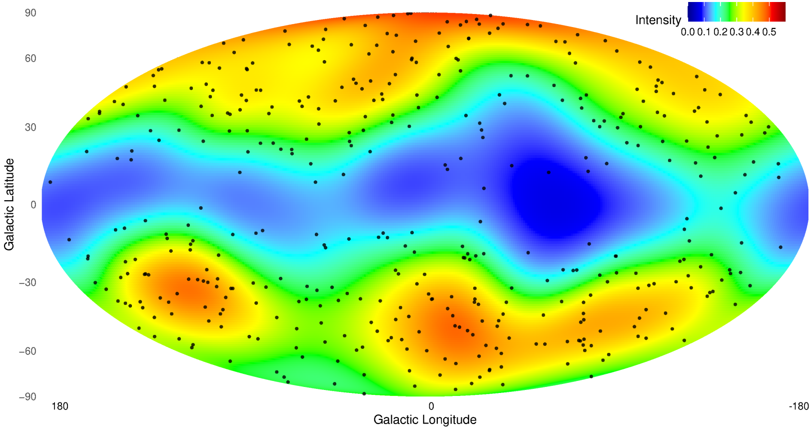

Preconditioned density estimate $\lambda_z(\mathbf{x}) = \lambda_{total}(\mathbf{x}) \times P(z|\mathbf{x})$ for the Lumped model. It is better; the Split model is statistically inferior because of overfitting.

Are there any Subgroup Probability Map Differences?

Surprise: The Lumped Completeness Map is better than the Split One!

One would not expect the Afterglow and the Host Galaxy subgroups to have the same Precon Maps!

- **Afterglow:** Rapid response, sensitive to atmospheric conditions and daytime triggers. Prompt access of the telescopes/observers/equipment/TOO is important!
- **Host Galaxy:** Delayed observation, sensitive to galaxy brightness and stellar crowding in the Galactic Plane. High-exposure, limited by telescope magnitude limits. Sometimes years/decades later than the gamma detection, observational campaigns are common!

The timeline is totally different!

Is there any real difference?

Precon density estimate prefers the Lumped model, but does any other statistical positional test discriminate between the two subgroups?

Are there any Subgroup P

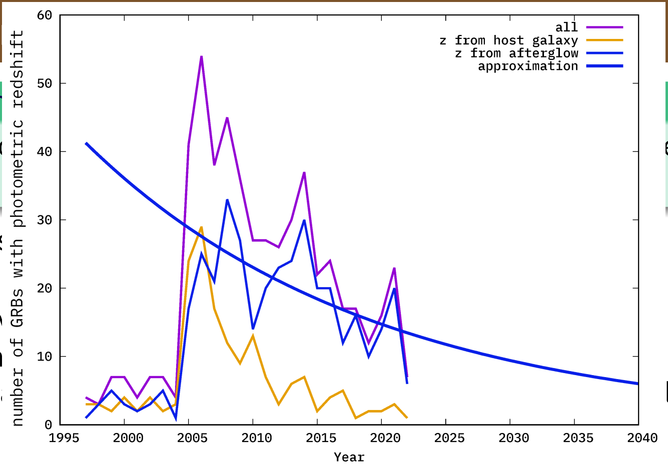

Surprise: The Lumped Completer

One would not expect the Aftergl e
Precon Maps!

- **Afterglow:** Rapid response, s
triggers. Prompt access of th nt!
- **Host Galaxy:** Delayed observ
crowding in the Galactic Plan
limits. Sometimes years/deca l
campaigns are common!

The timeline is totally different!

Observation timeline is *different* for Host Galaxy/Afterglow groups!

Is there any real difference?

Precon density estimate prefers the Lumped model, but does any other statistical positional test discriminate between the two subgroups?

Testing the Afterglow/Host Galaxy Relative Sky Distribution

Comprehensive suite of spherical statistics

A **Spherical Cross-Nearest Neighbor** (Local clustering).
B **Maximum Mean Discrepancy (MMD)** (Distributional distance).
C **Spherical Ripley's K-Function** (Multi-scale correlation).
D **Fasano-Franceschini Test** (2D Kolmogorov-Smirnov).
E **Monte Carlo Predictive Likelihood Inversion** (Global structure).

Generate random catalogs with random splits of the Afterglow/Host Galaxy data.

Test A: Nearest Neighbor Distances

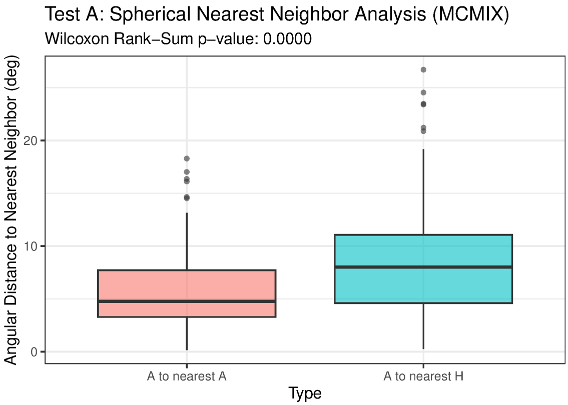

Initial test shows significant difference ($p < 0.0001$) for the real data!

This is a cardinality artifact!
Samples with different densities always have different neighbor distances.

Test A: Nearest Neighbor Distances with Rarefaction

To fix the density bias we randomly sub-sample the Afterglow group to $n = 127$, repeated 10,000 times.

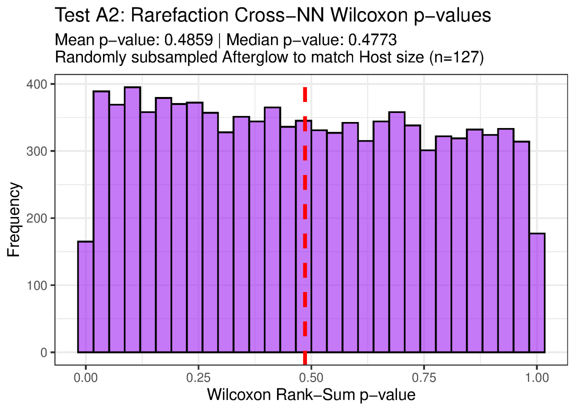

The significance disappears after rarefaction.

Test B: Maximum Mean Discrepancy (MMD)

Theoretical Context

MMD measures the distance between probability embeddings in a Hilbert Space.

$$\mathrm{MMD}^2 \propto \sum K(x_i, x_j) + \sum K(y_i, y_j) - 2 \sum K(x_i, y_j)$$

MMD: Choice of Kernel and Scale on a Sphere

- Isotropic Gaussian kernel on the sphere ($\sigma = 15^\circ$)
  $\rightarrow$ characteristic scale of instrumental modulation ($\approx 11.7^\circ / 18^\circ$ average distances for Afterglow/Host Galaxy events).
- Gaussian kernel is symmetric and positive-definite on the sphere for small σ.
- Calculated at $N = 196608$ Healpix centers.

Test B: MMD Result

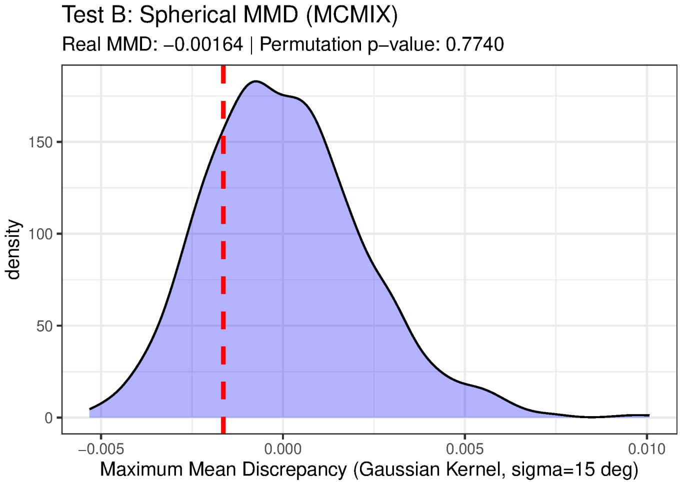

Observed MMD is almost in the center of the null distribution ($p = 0.77$).

Test C: Spherical Ripley's K-Function

$$\hat{K}(\theta) = \frac{\text{Area}}{n(n-1)} \sum \sum \mathbb{I}(dist < \theta)$$

Compares clustering behavior at all angular scales simultaneously.

Ripley's K: Expected vs. Observed

- For a Poisson process: $K(\theta) = 2\pi(1 - \cos\theta)$.
- Deviations indicate clustering or repulsion.

Test C: Ripley's K Result

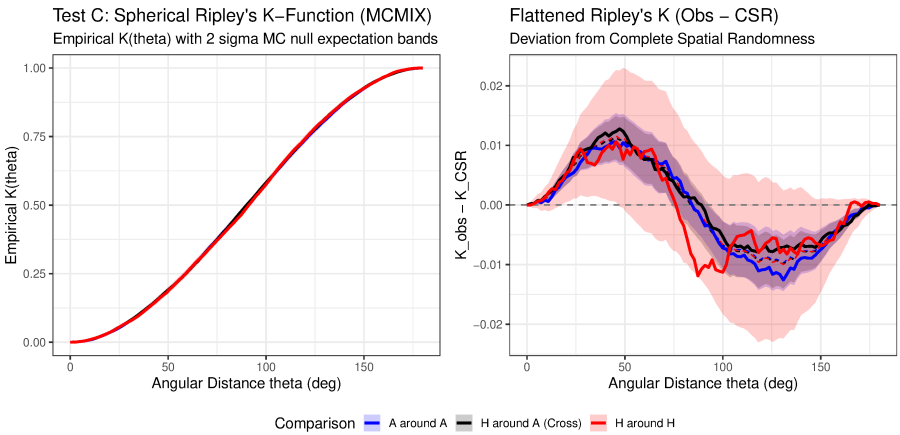

Auto- and cross-correlation functions with 2σ error bands. A global clustering structure can be observed at angular scales of $\approx 40° - 50°$.

All empirical distributions are within the 2σ expectations.

Test D: Fasano-Franceschini 2D KS-Test

Two-dimensional extension of the Kolmogorov-Smirnov test

Divide the plane into four quadrants $Q_1^{(i)}$ to $Q_4^{(i)}$ around point i :

$$f_A^{(i,q)} = \frac{1}{n_A} \sum_{j \in A} \mathbb{I}\left((\Delta l_j, \Delta b_j) \in Q_q^{(i)} \right), \quad f_H^{(i,q)} = \frac{1}{n_H} \sum_{k \in H} \mathbb{I}\left((\Delta l_k, \Delta b_k) \in Q_q^{(i)} \right)$$

$$D = \max_{i \in \{1 \ldots n\}} \max_{q \in \{1,2,3,4\}} \left| f_A^{(i,q)} - f_H^{(i,q)} \right|$$

- Analyzes cumulative fractions in quadrants around each point.
- Sensitive to directional gradients.
- Maximum absolute difference D over all points.
- $(\Delta l, \Delta b)$ spherical wraparound: four quadrants based on the local horizon, Local North + Local East

Test D: Fasano-Franceschini Result

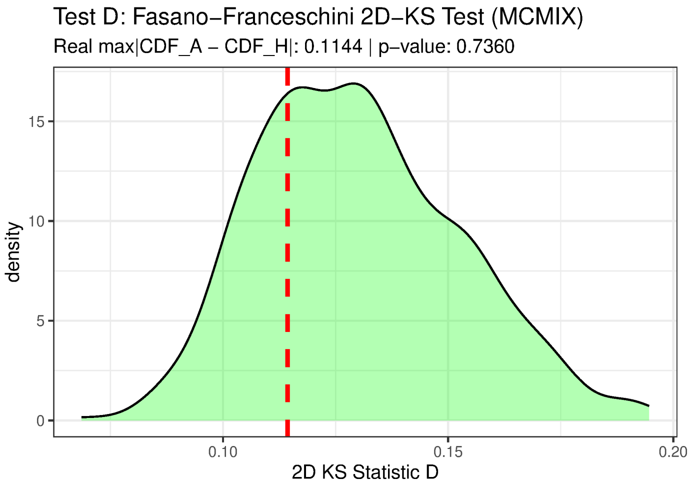

Maximum deviation is non-significant ($p = 0.736$).

Test E: Global Likelihood Comparison

We compare the **Lumped Model** (one surface) against the **Split Model** (sum of two surfaces), using the Precon model and random catalogs.

- Measured $\Delta\mathcal{L} = -18.84$.
- Negative value indicates that splitting the sample causes overfitting.

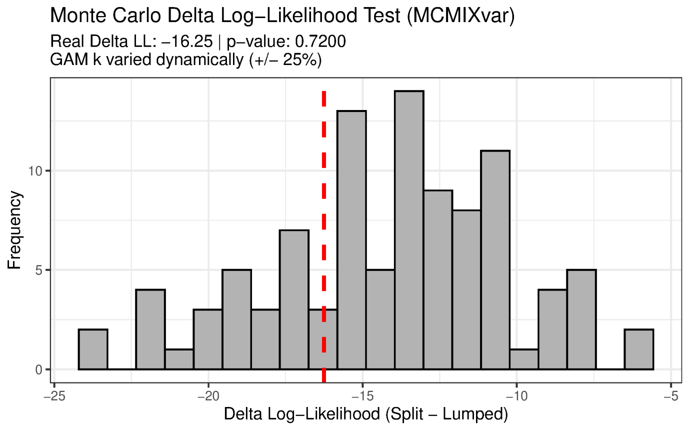

The observed difference is consistent with a single population.

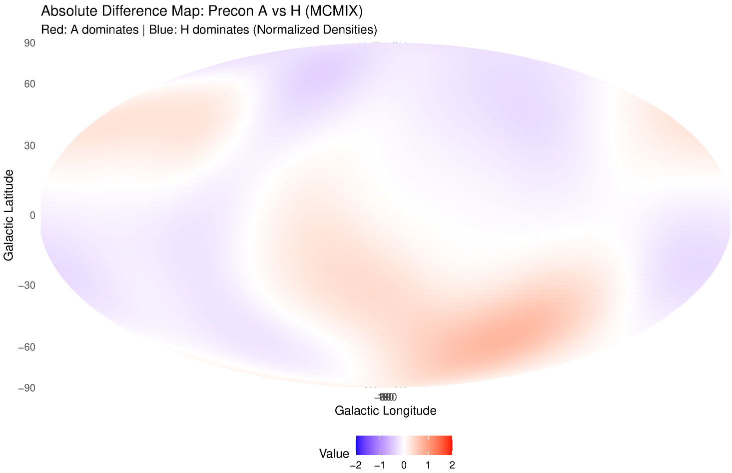

Absolute difference between normalized subgroup densities.

Test E: Global Likelihood Relative Difference Map

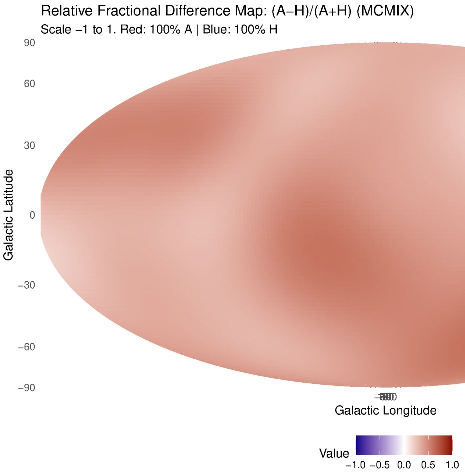

Highlights deviations in low-exposure regions.

Subgroup Structures: Afterglow Completeness Map (compare!)

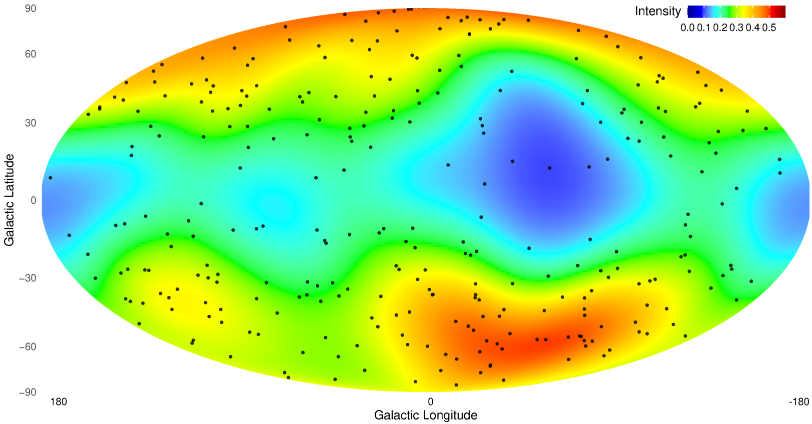

Afterglow $\lambda_z(\mathbf{x}) = \lambda_{total}(\mathbf{x}) \times P(z|\mathbf{x})$ map for $k = 41$

.

Subgroup Structures: Host Galaxy Completeness Map (compare!)

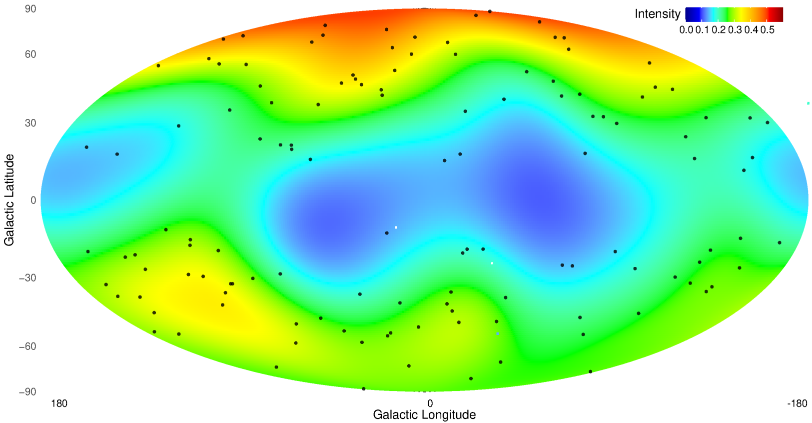

Host Galaxy $\lambda_z(\mathbf{x}) = \lambda_{total}(\mathbf{x}) \times P(z|\mathbf{x})$ map is smoother ($k = 23$) due to lower statistics ($N = 127$).

Test E: Global Likelihood Sigma Significance Map

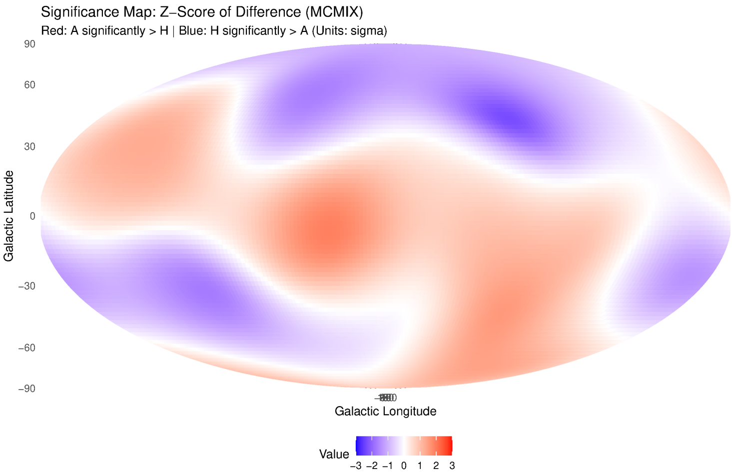

No region exceeds the 3σ threshold.

Conclusions

Precon Estimator

- Distinguishes physical clustering from observational bias.
- The framework depends only on having a ”Total” catalog and a ”Selected” subset.
- Corrects for sky exposure variance induced by satellite mechanics.
- Creates a noise-filtered background for identifying true structures (e.g., Giant Ring, Great Wall).

Statistically Identical Sky Distributions for Afterglow and Host-Galaxy GRBs!

Sky Exposure is Compatible!

- Directly applicable to current/upcoming missions (**SVOM**, **Einstein Probe**, **THESEUS**).
- Raises the open question of whether coordinate-dependent completeness weights should be incorporated into luminosity function and rate density calculations.

Summary

1. **Methodology:** Bayesian Preconditioned Estimator for Completeness Function.
2. **Performance:** Outperforms AKDE by Bayes Factor $> 10^{30}$.
3. **Physics:** Recovers high-frequency features beyond the Nyquist limit.
4. **Stability:** Proves sky exposure compatibility of Afterglow / Host Galaxy subpopulations.

Acknowledgments

Support: TKP2021-NVA-16 and TKP2021-NKTA-64.
Data: Neil Gehrels Swift Observatory and UKSSDC.
Code: Uses CRAN R ‘mgcv‘ and ‘sphereplot‘. The developed code implements full spherical geometry and is available at
`https://github.com/zbagoly/GRBPreconMap`.

Questions?

Final Conclusion

Bayesian Preconditioning provides a
statistically rigorous
and
physically robust
way to estimate
Completeness Functions.